# Kinematic Analysis for a Prostate Biopsy Parallel Robot using Study parameters

**I. Birlescu[1], P. Tucan[1], B. Gherman[1], C. Vaida[1], N. Crisan[2], C. Radu[2], N. Plitea[1] and D. Pisla[1*]**

[1] *CESTER, Technical University of Cluj-Napoca, Romania 400114 Memorandumului 28, e-mail: doina.pisla@mep.utcluj.ro*

[2] *Iuliu Hatieganu University of Medicine and Pharmacy, Cluj-Napoca, Romania, e-mail: nicolae.crisan@umfcluj.ro*

*Corresponding author



**Abstract**. The paper presents the forward kinematics computation for a parallel robotic system designed for prostate biopsy using Study parameters. The manipulator is analyzed on its smaller kinematic chains to facilitate the computation, in a way that no information is lost from the robotic system functionality. Kinematic solutions examples are presented based on numerical values given for the robot geometric parameters and active joint position.

**Key words:** Parallel robot, Study parameters, Forward kinematics.

## 1 Introduction

Computations regarding the kinematics and singularities of robotic structures are of great interest since they provide valuable information about the manipulator functionality. This information has the capability to reduce the risk factor of using a robotic structure in various procedures, which is especially important in medical applications where the patient and medical staff safety is a priority [1]. Image guided prostate biopsy is one procedure where the benefit of using a robotic system outweighs the risk [1,2]. One particular way to access the prostate tissue is transperineally, guided by a transrectal ultrasound (TRUS) probe inserted into the patients' rectum, were the advantages are that the entire prostate volume can be sampled, and lesser infection risk [3,4,5].

The focus of this paper is the computation of the forward kinematics of the BIO – PROS 3 robotic system, using Study parameters. BIO – PROS 3 robotic system kinematics and singularities were studied in previous work, using a classical method where the kinematics are derived from the robot geometric model, and the singularities are studied from the vanishing points of the determinants of the Jacobi matrices A and B [4]. It has been pointed out in [6] that the singularity analysis using the Study parameters method may provide more singular configurations than the analysis of the Jacobi matrices. Study parameters method for solving the forward kinematics, parameterize the Euclidean displacement using quaternions, and computes a set of 8 parameters as shown in [7,8,9]. Computations based on the method were done to describe mechanisms such as: the Stewart-Gough platform [7], 3-RPS manipulator [8], and a medical robot (PARA-BRACHYROB) for brachytherapy [6].

The complexity of the BIO-PROS 3 robot did not allow the kinematic computation of the whole mechanism using the Study parameters. As an alternative, a geometric parameter was introduced, in a way that the kinematic results were not affected, but Maple managed the computation.

The following sections of this paper are structure as follows. Section 2 presents the BIO – PROS 3 robotic system, and the forward kinematics computation using Study parameters, and illustrates examples based on numerical values (for active joints and structural parameters). Section 3 presents the conclusions and proposed further research.

# 2 BIO-PROS 3 parallel robot

BIO-PROS 3 is a robotic system (Fig. 1) from the parallel robots family [10] designed for transperineal prostate biopsy, which contains two independent modules, one for biopsy gun guidance (Fig. 2.a), and one for transrectal ultrasound (TRUS) probe guidance (Fig. 2.b) [4]. For transperineal prostate biopsy the insertion of both TRUS probe and biopsy needle follow a linear path (±10$^o$ needle angulation is preferred relative to TRUS probe insertion axis [2]). The positioning and insertion of the TRUS probe is achieved by the module active joints, while for the biopsy gun, the position is obtained by the module active joints and the needle insertion is realized with a redundant DOF from an insertion instrument (such as [5]) to increase precision.

## *2.1 Robotic system description*

Each module has 5 active joints, $q_i$ for the TRUS probe guiding module, and $q'_i$ for the biopsy gun guiding module, which leads in turn to 5 DOF manipulators. By defining a fixed coordinate frame OXYZ placed in the robotic systems base (see Fig. 2), a moving frame O'X'Y'Z' is introduced (placed on the manipulators end effector). The two modules are similar in functionality and architecture, the difference being that the kinematic chain actuated by $q_{4\text{-}5}$ (of the TRUS guidance module) lies on a plane orthogonal to the plane in which $q_{1\text{-}3}$ are constrained, in opposition to the biopsy gun guiding module, where the kinematic chain actuated by $q'_{4\text{-}5}$ lies in the same plane with the active joints $q'_{1\text{-}3}$. For the TRUS guidance module, the end effector represents (mechanically speaking) a link between two cardan joints ($rf_1$ and $rf_2$ on Fig. 2), and its motion is obtained from the motion of a platform with constant orientation linked with $rf_1$, working in Cartesian coordinates (actuated by $q_{1\text{-}3}$), combined with the motion of a kinematic chain (linked in $rf_2$ and actuated by $q_{4\text{-}5}$) that works in cylindrical coordinates and has a free rotation $rf_0$ around an axis defined by the translation axis of both active joints $q_{4\text{-}5}$ (see Fig.3).

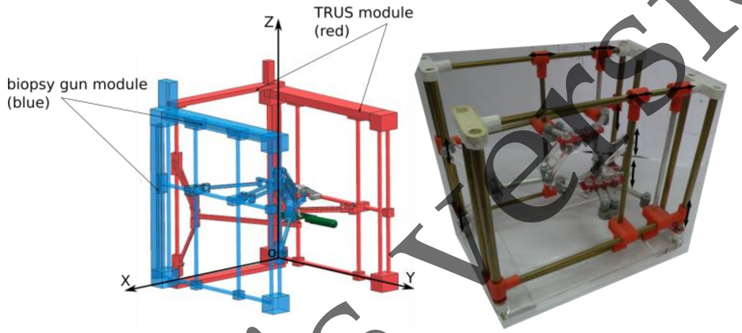


Fig. 1 BIO-PROS 1 parallel robot CAD representation [4] on left; 3D printed model on right.

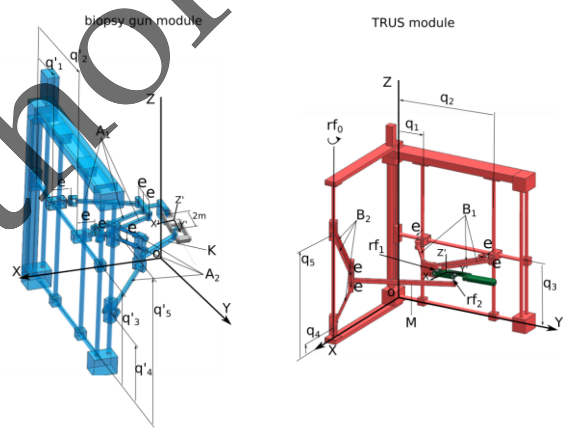


Fig. 2 BIO-PROS 3; biopsy gun module on left; TRUS module on right.

## 2.2 Forward kinematics

Study parameters are used to compute the forward kinematics of the robotic system, since the Study method is free of parameterization singularities [6]. Two distinct kinematic chains are defined (chain 1 and chain 2) that intersect in the mobile coordinate frame O'X'Y'Z' (for each module) as shown in Fig. 3. The kinematic chain 1 has at its basis a type R-2PRR mechanism with 3 DOF (one being a free rotation), and the kinematic chain 2 is type P-2PRR with 3 translational DOF.

A computation of the kinematics regarding the whole mechanism (as sketched in Fig. 3.a) was not possible in Maple using an Intel i7 3.6 GHz with 16 GB of RAM computer configuration. For this reason, the computation was performed on separated kinematic chains as described further in this section. Figure 3.b illustrates the simplest way to sketch the kinematics of the manipulator by taking into account how each joint influences the mobile coordinate frame position and orientation. Since a point N(x,y,z)=f($q_1$,$q_2$,$q_3$) (fixed on the platform with constant orientation) is introduced as a way to facilitate the computation, Fig. 3.b illustrates the kinematics of both TRUS and biopsy gun modules. Were D represents a displacement on X and Y axes for the needle module, and a displacement on X for the TRUS module. Hereafter the paper is focused on describing the TRUS module since the computation is identical for both modules.

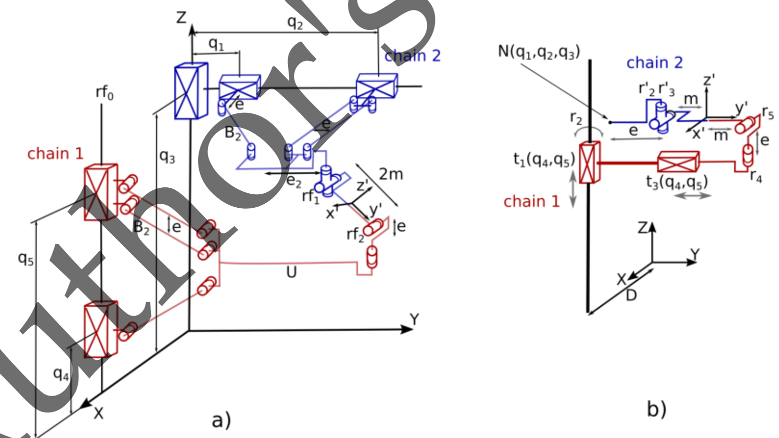


Fig. 3 Kinematic representation of BIO-PROS 3.

To find the Study parameters of a moving frame O'X'Y'Z' relative to the fixed frame OXYZ, the Denavit–Hartenberg (DH) parameters are written for each joint/link, and the matrices are multiplied to obtain the constraint conditions:

$$\begin{aligned} C_1 &= Td \cdot T_1 \cdot R_2 \cdot T_3 \cdot R_4 \cdot Te \cdot R_5 \cdot M \\ C_2 &= N \cdot Te' \cdot R'_2 \cdot R'_3 \cdot M' \end{aligned} \quad (1)$$

Table 1 contains the parameters for each DH matrix transformation, where $r_i$ (and $r'_i$) represent free rotation parameters derived from the $R_i$ (and $R'_i$) using the half angle tangent formulae.

From $C_1$ and $C_2$ the Study parameters are computed (as described in [7]) yielding Eq. (2) and (3). Regarding Study parameters as algebraic varieties, two polynomial ideals are generated, *I* for Eq. (2) and *I'* for Eq. (3). Maple software was not able to generate a Gröbner basis for *I* (on the computer previously mentioned), therefore the linear implicitization algorithm (also used in [9]) was used before computing a Gröbner basis *G*.

**Table 1.** Parameters for the DH transformation matrices

| *C1/ C2* | *Parameter* | *Description* | *Type* |
|---|---|---|---|
| Td / N | dx/Xn,Yn Zn | displacement on X / XYZ | geometric parameter / active translation |
| $T_1$ | $t_1$ | displacement on Z | active translation |
| $R_2$/ $R'_2$ | $r_2$/$r'_2$ | rotation around Z | free rotation |
| $T_3$/Te' | $t_3$/$e_2$ | displacement on Y | active translation / geometric parameter |
| $R_4$ | $r_4$ | rotation around Z | free rotation |
| Te | e | displacement on Z | geometric parameter |
| $R_5$/$R'_3$ | $r_5$/$r'_3$ | rotation around X | free rotation |
| M /M' | m | displacement on Y | geometric parameter |

$$\begin{bmatrix} x_0 \\ x_1 \\ x_2 \\ x_3 \\ y_0 \\ y_1 \\ y_2 \\ y_3 \end{bmatrix} = \begin{bmatrix} 2\cdot r_2 - 2 \\ 2(r_2\cdot r_4 - 1)r_5 \\ -2(r_4 + r_2)r_5 \\ -2(r_4 + r_2) \\ r_2(r_5\cdot dx\cdot r_4 - t_1 - e + m\cdot r_5 + t_3\cdot r_5) + r_4(-t_1 - e + m\cdot r_5 - r_5\cdot t_3) - dx\cdot r_5 \\ r_2(dx\cdot r_4 - t_1\cdot r_5 + m - e\cdot r_5 - t_3) + r_4(-e\cdot r_5 + t_3 + m - r_5\cdot t_1) + dx \\ r_2(e\cdot r_5\cdot r_4 + t_3\cdot r_4 + m\cdot r_4 - r_5\cdot r_4\cdot t_1 - dx) - dx\cdot r_4 + r_5\cdot t_1 - m + e\cdot r_5 + t_3 \\ r_2(-t_1\cdot r_4 - e\cdot r_4 + m\cdot r_4\cdot r_5 - r_5\cdot t_3\cdot r_4 + r_5\cdot dx) + r_5\cdot r_4\cdot dx + e - r_5\cdot m + t_1 - t_3\cdot r_5 \end{bmatrix} \tag{2}$$

$$\begin{bmatrix} x'_0 \\ x'_1 \\ x'_2 \\ x'_3 \\ y'_0 \\ y'_1 \\ y'_2 \\ y'_3 \end{bmatrix} = \begin{bmatrix} 2 \\ 2r'_3 \\ 2r'_2\cdot r'_3 \\ 3r'_2 \\ r'_3\cdot r'_2\cdot Yn + m\cdot r'_3\cdot r'_2 + r'_2\cdot r'_3\cdot e_2 + Xn\cdot r'_3 + r'_2\cdot Zn \\ r'_2\cdot r'_3\cdot Zn - e_2\cdot r'_2 - Yn\cdot r'_2 + m\cdot r'_2 - Xn \\ -r'_3\cdot Zn + r'_2\cdot Xn - e_2 - Yn - m \\ -r'_2\cdot r'_3\cdot Xn + Yn\cdot r'_3 + r'_2\cdot r'_3 - r'_3\cdot m - Zn \end{bmatrix} \tag{3}$$

In the case of *I'* Maple returned a Gröbner basis (denoted *G'*). The mentioned Gröbner bases contain polynomials with Study parameters as variables. Solutions for the forward kinematic problem must be solutions both *G* and *G'*. Maple was able to compute a basis $G^*$ with the information from both *G* and *G'* after providing numerical values for some geometric parameters (in this example e=10, $e_2$=10, dx=350, m=50). The basis $G^*$ has a univariate polynomial (in $x_3$) of degree 8. By inputting numerical values for the active joints in G* and solving for $x_i$:$y_i$, numerical values for Study parameters are obtained. For a numerical example the following values were used: {$t_1$=100, $t_3$=300, Xn=300, Yn=250, Zn=120}; all the dimensions are expressed in mm. The computation yields 8 solutions but only 4 are of interest (the other 4 the first 4 multiplied by -1). The numerical values obtained are included in Table 2, and a kinematic representation of two solutions is illustrated in Fig. 4. The other two solutions represent the same displacement but with different orientation (a rotation around Z' axis combined with a rotation around X' axis by a value of π).

**Table 2.** Numeric solutions for Study parameters

| $x_0$ | $x_1$ | $x_2$ | $x_3$ | $y_0$ | $y_1$ | $y_2$ | $y_3$ |
|---|---|---|---|---|---|---|---|
| -0.035 | 0.705 | -0.706 | 0.035 | -0.151 | -4.080 | -3.155 | 18.222 |
| 0.028 | -0.559 | -0.827 | 0.414 | -20.968 | -5.819 | 3.545 | 6.361 |
| -0.827 | 0.041 | -0.028 | 0.559 | 3.545 | 6.361 | 20.968 | 5.819 |
| 0.706 | -0.035 | -0.035 | 0.705 | 3.155 | -18.222 | -0.151 | -4.080 |

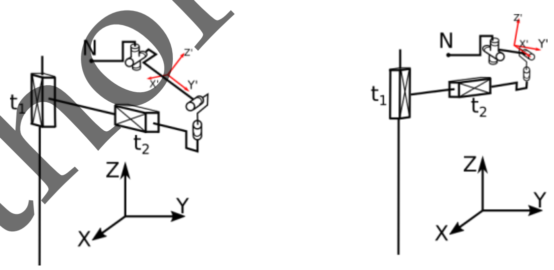


Fig. 4 Solutions for the forward kinematic problem.

Since a generalization was used to compute the forward kinematics (using the simplest kinematic representation illustrated in Fig. 3.b), the forward kinematics for the 2PRR mechanism is also computed using Study parameters. Following the kinematic representation from Fig. 5, the Study parameters were computed (after multiplying the matrices according to DH parameters) for three kinematic paths (illustrated as a,b,c in Fig. 5) yielding the Study parameters denoted $x_i^{a,b,c}$:$y_i^{a,b,c}$ (Eq. 4-7).

After computing three Gröbner bases (one for each ideal generated by Study parameters $x_i^{a,b,c}$:$y_i^{a,b,c}$) Maple Software was able to compute a base that contain the information from all three previous bases. Six distinct solutions, four of them being real (the remaining 2 complex solutions are not of interest) were returned after the following numerical values were input in the computation: {$q_1$=100, $q_2$=200, $q_3$=100, $B_1$=150, e=10}. Table 3 displays the numerical values for the solutions, and Fig. 6 illustrates a sketch of these solutions (with only solution 1 being of interest due to the robot functionality).

$$\begin{bmatrix} x_0^{a,b,c} \\ x_1^{a,b,c} \\ x_2^{a,b,c} \\ x_3^{a,b,c} \\ y_0^{a,b,c} \\ y_1^{a,b,c} \\ y_2^{a,b,c} \\ y_3^{a,b,c} \end{bmatrix} = \begin{bmatrix} 2 \cdot r_4 \cdot r_5 - 2 \\ 0 \\ 0 \\ 2 \cdot t_4 - 2 \cdot t_5 \\ -(r_5 + r_4) q_3 \\ y_1^{a,b,c} \\ y_2^{a,b,c} \\ -(r_4 \cdot r_5 - 1) q_3 \end{bmatrix} \tag{4}$$

$$\begin{aligned} y_1^a &= (B_1 r_5 - 2 e r_5 - e + q_1) r_4 - e r_5 + q_1 r_5 + 2e + B_1 \\ y_2^a &= (-q_1 r_5 - e r_5 + B_1) r_4 + q_1 + e - r_5 B_1 \end{aligned} \tag{5}$$

$$\begin{aligned} y_1^b &= (B_1 r_5 - 2 e r_5 - e + q_2) r_4 - e r_5 + q_2 r_5 + 2e + B_1 \\ y_2^b &= (-q_2 r_5 + e r_5 + B_1) r_4 + q_2 - e - r_5 B_1 \end{aligned} \tag{6}$$

$$\begin{aligned} y_1^c &= (B_1 r_5 - 2 e r_5 - 3e + q_2) r_4 - 3 e r_5 + q_2 r_5 + 2e + B_1 \\ y_2^c &= (-q_2 r_5 + e r_5 + B_1) r_4 + q_2 - e - r_5 B_1 \end{aligned} \tag{7}$$

**Table 3.** Numeric solutions for Study parameters for the 2PRR mechanism

| $x_0$ | $x_1$ | $x_2$ | $x_3$ | $y_0$ | $y_1$ | $y_2$ | $y_3$ |
|---|---|---|---|---|---|---|---|
| 1 | 0 | 0 | 0 | 0 | -82.284 | -75 | -100 |
| 1 | 0 | 0 | 0 | 0 | 62.284 | -75 | -100 |
| 0.510 | 0 | 0 | -0.859 | -85.970 | 85.161 | 26.351 | -51.079 |
| 0.510 | 0 | 0 | 0.859 | 85.970 | -95.376 | 26.351 | -51.079 |

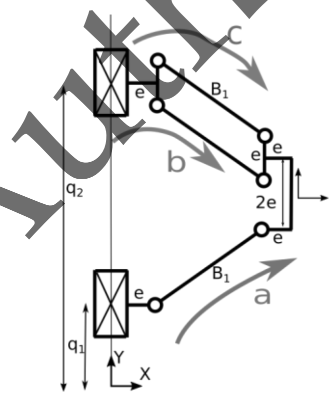


Fig. 5 Kinematic sketch for the 2PRR mechanism

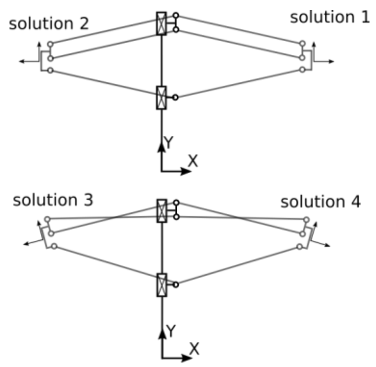


Fig. 6 Kinematic solutions for the 2PRR mechanism

# 3 Conclusions

The forward kinematics computation presented in this paper was conducted using Study parameters. Due to computing limitations the manipulator kinematic chains were treated independently but no global information of the manipulator functionality was lost. A detailed (mathematically speaking) representation of kinematic solutions was presented, with two possible (mechanically speaking) solutions for the manipulator, and one possible solution for the 2PRR mechanism. Based on the results of this paper, future research is planned to achieve a complete singularity analysis using Study parameters. Furthermore, the inverse kinematics analysis is planned, in order to practically validate the robotic system for its particular task (transperineal prostate biopsy under TRUS guidance).

**Acknowledgments** This paper was realized within the Partnership Programme in priority domains - PN-II, which runs with the financial support of MEN-UEFISCDI through Project no. 247/2014, code PN-II-PT-PCCA-2013-4-0647 – ROBOCORE and also the Project no 59/2015, code PN-II-RU-TE-2014-4-0992 – ACCURATE.

# References

1. Tarun, K. P. et al.: AAPM and GEC-ESTRO guidelines for image-guided robotic brachytherapy: Report of Task Group 192. Am. Assoc. Phys. Med. (2014)
2. Stoianovici, D. et al.: MRI Stealth robot for prostate interventions. Minim Invasive The Allied Technol; 16(4): 241248 (2007)
3. Chang, D., Challacombe, B., Lawrentschuk, N.: Transperineal biopsy of the prostate-is this the future?. Nature Reviews Urology (September 2013)
4. Gherman, B., Plitea, N., Pisla, D.: "An Innovative Parallel Robotic System for Transperineal Prostate Biopsy", New Trends in Mechanism and Machine Science, Mechanisms and Machine Science, 43, pp. 421-429 (2017)
5. Vaida, C. et al.: Design of a Needle Insertion Module for Robotic Assisted Transperineal Prostate Biopsy. MESROB 2016 - 5th International Workshop on Medical and Service Robots, Graz Austria (July 2016)
6. Vaida, C., Pisla, D., Schadlbauer, J., Husty, M., Plitea, N.: Kinematic Analysis of an Innovative Medical Parallel Robot Using Study Parameters. New Trends in Medical and Service Robots. Mechanisms and Machine Science, vol 39. Springer, pp. 85-99 (2016)
7. Husty, M., Pfurner, M., Schroecker, H.P., Brunnthaler, K.: Algebraic Methods in Mechanism Analysis and Synthesis. Robotica, vol 25, Issue 6, pp. 661-675 (November 2007)
8. Husty, M., Schroecker, H.P.: Algebraic Geometry and Kinematics. Nonlinear Computational Geometry, vol 151, pp. 85-107 (October 2009)
9. Schadlbauer, J., Walter, D.R., Husty, M.: The 3-RPS parallel manipulator from an algebraic viewpoint. Mechanism and Machine Theory, vol 75, pp. 161176 (January 2014)
10. Plitea, N., Pisla, D., Vaida, C., Gherman, B., Tucan, P., Covaciu, F.: Family of innovative parallel robots for transperineal prostate biopsy, Patent pending: A/00191/13.03.2015